Pseudo-Elliptic Bandpass Filters Using Closed-Loop Resonator

Norfishah Ab. Wahab[#1], I. Pasya[#2], M. F. Abdul Khalid[#3], I. M. Yassin[#4], S. H. Herman[#5], Z. Awang[#6]

 # Microwave Research Institute, Universiti Teknologi MARA, 40450 Shah Alam, Selangor, Malaysia
E-mail: [1]norfishah@ieee.org, [2]idnin@salam.uitm.edu.my, [3]mfarid044@salam.uitm.edu.my, [4]ihsan.yassin@gmail.com,
[5]hana1617@salam.uitm.edu.my, [6]zaiki437@salam.uitm.edu.my

Abstract— **2nd order pseudo-elliptic resonator topologies are presented in this paper. Based on the closed loop with coupled-line resonator, three 2nd order bandpass filter topologies were built. Each of these topologies offered pseudo-elliptic bandpass response with high selectivity that is suitable for RF and wireless applications. The main advantage of these topologies is that the structures were built from a closed-loop with coupled-line resonator which is easy to control to obtain desired electrical responses. To demonstrate the proposed concepts, the resonators were realized using microstrip technology and all the measurement results showing good agreement with those from the simulations.**

Keywords— **bandpass filter; coupled-line; meander lines, miniaturized; pseudo-elliptic; resonator**

I. INTRODUCTION

Pseudo-elliptic bandpass filters have been widely implemented in radio channels frequency separation for their high selectivity characteristic [1]-[3]. Features like compact, simple to design, easy to fabricate and low loss bandpass filters are also the main key points to the filter design in meeting the rigorous and modern wireless and RF communication system [4], [5].

Other than that, miniaturization of RF passive components has also been required constantly for the development of low-cost communication system [6]-[8]. Above all things, transmission line should be miniaturized to reduce the size of RF components, since the distributed RF components basically consist of transmission line [9-10]. To mention a few, meander lines have been widely used to achieve compact transmission line. This is due to its small layout area, in which enabled a reduction of chip size [11], [12].

In this paper, three arrangements of bandpass filters were proposed using the closed-loop with coupled-line structure [13]. The first resonator made use of the closed-loop, and new additional coupled-line was introduced at the end of the existing coupled-line. This resonator when simulated gave a reasonable fractional bandwidth of less than 20%. The second resonator was built based on the same closed loop with coupled-line, but in this arrangement, the coupled-line is a sandwich in between the two closed-loop lines. In terms of fractional bandwidth, the second resonator gives smaller bandwidth compared to the first resonator. The third resonator was proposed to reduce the size of the second topology. In this work, meander lines were proposed to reduce the overall size of the resonator.

All the proposed ideas were tested through simulations using full wave electromagnetic simulation tool, performed on microstrip substrate at the resonance frequency of 2 GHz. The entire proposed filters show low insertion loss of less than 3dB while the return loss exceeds 10 dB.

II. MATERIAL AND METHOD

A. Topology 1: Single Closed-loop with Second Coupled-Line

In this section, the topology of closed-loop resonator and its electrical response are presented as shown in Fig. 1(a) and 1(b) respectively. This topology exhibits a pseudo-elliptic bandpass filter response with single resonance at the center frequency, f_o while two transmission zeros at the lower and upper stopbands with attenuation more than 30 dB for high selectivity. With three parameters to controlled to obtain desired response, the topology is flexible and can be used as a base cell in developing higher order filters. Various techniques can be applied to achieve this [13]. Indeed, to increase the number of modes of a filter, resonators can be introduced to the existing structure, and this can actually be easily realised.
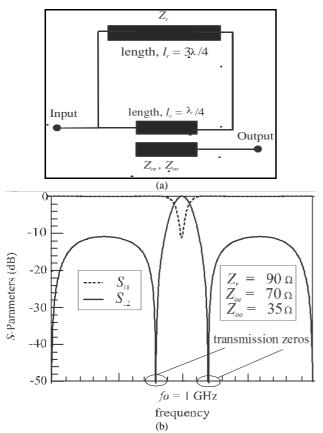
(a)

(b)

Fig. 1   A pseudo-elliptic closed-loop resonator: (a) Topology, (b) Ideal response of the resonator [13]

In this work, the closed-loop with a quarter-wavelength coupled-line resonator in Fig. 1(a) was chosen as the base cell to built 2nd order bandpass filters. The characteristics of the newly 2nd order bandpass filters were then investigated in terms of insertion loss, return loss and bandwidth to distinguish the suitability of the implementation of the filters in RF applications. Various techniques were explored such as introducing new coupled line or cascading the basic cells. In the first technique, the basic cell was cascaded with a second quarter-wavelength coupled-line via its output feed-line to form a 2nd order bandpass filter.

As illustrated in Fig. 2, the impedances using this configuration can easily be determined by optimizing the circuit using full wave electromagnetic simulator. All the values of the impedances are summarized in Table 1 with new parameters for the second coupled-line, denoted as Z_{oo1} and Z_{oe1} were introduced here. All the impedance values were chosen to be in the accepted range for microstrip technology.

TABLE I
TOPOLOGY 1: IMPEDANCES OF THE CLOSED-LOOP WITH SECOND COUPLED-LINE, DESIGNED AT 2 GHZ

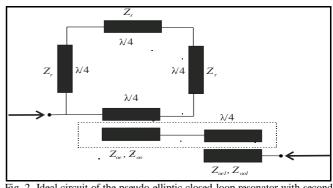| Parameter	Value (Ω)
Even-mode impedance of the coupled-line, Z_{oe}	70
Odd-mode impedance of the coupled-line, Z_{oo}	40
Impedance of the closed-loop line, Z_r	112
Even-mode impedance of the second coupled-line, Z_{oe1}	116
Odd-mode impedance of the second coupled-line, Z_{oo1}	60

Fig. 2   Ideal circuit of the pseudo-elliptic closed-loop resonator with second coupled-line
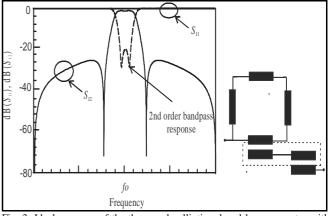

Fig. 3   Ideal response of the the pseudo-elliptic closed-loop resonator with second coupled-line
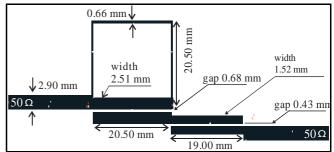

Fig. 4   Layout of the microstrip pseudo-elliptic closed-loop with second coupled-line bandpass filter

The circuit was simulated, and as shown in Fig. 3, the response of the ideal circuit demonstrates a pseudo-elliptic 2nd order bandpass response. It can be seen that two poles were obtained in the passband, resonated at 1.915 GHz and 2.089 GHz giving separation of 0.174 GHz. Two transmission zeros frequencies were found; 1.533GHz for the lower-side stopband and 2.467 GHz for the upper-side stopband, resulted to the fractional bandwidth of 22.75 %.

Finally, for implementation purpose, the layout of the resonator was obtained as illustrated in Fig. 4. The dimensions of the first topology of the 2nd order bandpass filter are listed in Table 2. It shows that the lengths of both coupled-lines, L1 and L2 are 20500μm and 25100μm respectively; and are considered as a large size of filter. Meanwhile, the dimension of the coupling gap of the first couple-line is 680 μm while the second coupled line is 430 μm.

TABLE II
DIMENSIONS OF CHE CLOSED-LOOPS WITH SECOND COUPLED-LINE OF THE
2ND ORDER BANDPASS FILTER

Parameters	Dimensions (μm)
S1	680
L1	20500
L2	25100
W1	660
W2	2510
W3	1520
L3	1900
S2	430

B. Topology 2: Two-Closed-Loops Bandpass Filter Topology for Narrow Bandwidth Application
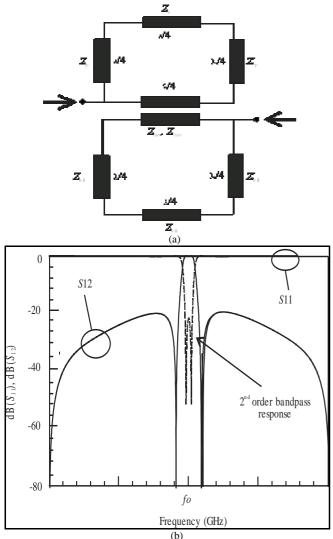

(a)

(b)

Fig.5 Ideal circuit of the 2 closed-loops pseudo-elliptic bandpass filter, (a) topology, (b) simulated response

TABLE III
TOPOLOGY 2: IMPEDANCES OF THE TWO-CLOSED-LOOPS OF THE 2ND ORDER
BANDPASS FILTER

Parameter	Value (Ω)
Even-mode impedance of the coupled-line, Z_{oe}	113
Odd-mode impedance of the coupled-line, Z_{oo}	75
Impedance of the first closed-loop, Z_r	162
Impedance of the second closed-loop, Z_{r1}	56

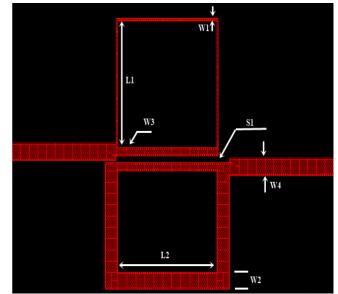Fig. 6 Layout with dimensions of the 2 closed-loops of the 2nd order bandpass filter

To enrich the filter banks, the basic closed-loop in Fig. 1 was further explored for the creation of second pseudo-elliptic 2nd order bandpass filter. In this arrangement, the basic cell is added with a new closed-loop line. It can be seen that the coupled-line is now placed in between the two closed-loops, while the circuit is powered via this coupled-line as illustrated in Fig. 5(a). The total circumference of each closed-loops is now equal to one wavelength at the operating frequency f_o. A quarter-wavelength parallel coupled line is placed at each side of the closed-loop. In this case, the elements of the new closed-loop line are not equal to the base cell's closed-loop line. Therefore, additional parameters of the newly closed-loop line need to be controlled for this higher-order designs as well. As illustrated in Fig. 5, the impedances of this configuration can easily be determined by optimizing the circuit using full-wave electromagnetic simulator. All the values of the impedances are summarized in Table 3 with new parameters for the second closed-loop line, denoted as Z_{r1} is introduced. Again, all the impedance values of this topology were chosen to be in the acceptable range for microstrip technology.

Next, the circuit was simulated, and the filter depicted the pseudo-elliptic frequency response with two poles in the passband region and two transmission zeros at the stopbands as shown in Fig. 5(b). As seen here, two poles in the passband were resonating at 1.960 GHz and 2.039 GHz to exhibit a separation of 79 MHz. Two transmission zeros frequencies were found to be very close to the cut-off frequencies, which are 1.818 GHz at the lower-side stopband and 2.182 GHz at the upper-side stopband to give a narrow passband bandwidth of 0.364 GHz. The cut-off frequencies of the passband occurred at 1.913 GHz and 2.089 GHz result to the fractional bandwidth of 8.80% which made the response very sharp, selective and suitable for narrow bandpass response.
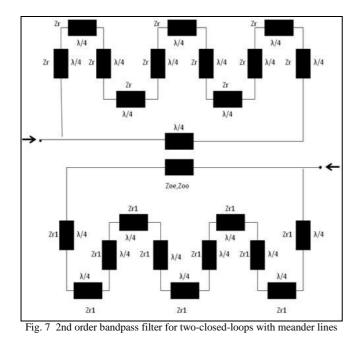
Finally, for implementation purpose, the layout of the resonator was obtained as illustrated in Fig. 6. The layout dimensions of the second topology of 2nd order bandpass filter listed in Table 4 shows that the length of both closed-
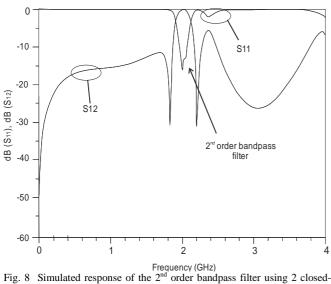
loops, L1 is 22000μm which is considered as a large size of filter. Meanwhile, the dimension of the coupling gap of the filter which is labelling as S1 is 1200μm. For a compact size filter, this topology can be further reduced in size by using meander line technique [8], [9].

TABLE IV
DIMENSIONS OF THE TWO-CLOSED-LOOPS OF THE 2ND ORDER BANDPASS FILTER

Parameters	Dimensions (μm)
S1	1200
L1	22000
L2	1760
W1	380
W2	2860
W3	1400
W4	2860

C. Topology 3: Miniaturised 2nd Order Bandpass Filter using Closed-Loop Meander Lines

Fig. 7 2nd order bandpass filter for two-closed-loops with meander lines

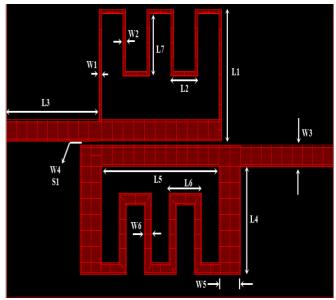Fig. 8 Simulated response of the 2nd order bandpass filter using 2 closed-loops with meander lines

Fig. 9 Layout with dimensions of the 2 closed-loops resonator with meander lines

TABLE V
DIMENSIONS OF THE TWO-CLOSED-LOOPS WITH MEANDER LINES FOR BANDPASS FILTER

Parameters	Dimensions (μm)
S1	300
L1, L4	11000
L2	3425
L3	15000
L5	19000
L6	2800
L7	6000
W1	380
W2	470
W3, W4	2200
W5	3460
W6	1250

Based on the parameters values in Table 5, the length of the top closed-loop, L1 is 11000μm with the gap coupling of 300μm. The gap is very much reduced now compared to the actual length of the second topology. The length of each meander lines of the top closed-loop is 3425μm while the length of each meander lines of the bottom closed-loop is 2800μm.

In this proposed resonator, meander lines were introduced to reduce the size of the second resonator in Fig. 6. Taking into account, the responses must be a pseudo-elliptic 2nd order bandpass filter with high selectivity; the lines must be carefully optimized so that the response can be maintained. Fig. 7 illustrates the third design of the 2nd order bandpass filter with both sides of the closed-loops are shaped in meander, and resonate at 2GHz center frequency for narrowband application. The topology is optimized using electromagnetic simulator to obtain desired response of pseudo-elliptic response.

This bandpass filter was then simulated using electromagnetic simulator and the simulation response was recorded. Fig. 8 illustrates the simulated response of the third pseudo-elliptic 2nd order bandpass filter topology. It can be seen that the resonance frequencies were at 1.981GHz and 2.142GHz. The 2nd order response is centred at 2GHz with

transmission zeros obtained at lower transmission zeros of 1.857 GHz and higher transmission zeros of 2.154 GHz. The insertion loss is obtained at 0.471 dB. The fractional bandwidth of this topology is 9.54%. The layout with simulated dimensions of the third 2nd order bandpass filter with meander lines is shown in Fig. 9.
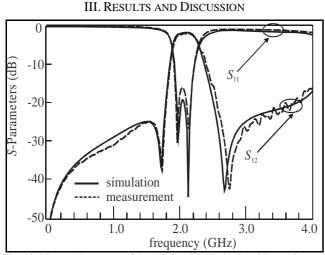
III. RESULTS AND DISCUSSION

Fig. 10 Measured response of the the pseudo-elliptic closed-loop with new coupled-line bandpass filter

Fig. 11 Fabricated photo of the the first topology base on the base cell with second coupled-line

For proof of concept, all the proposed resonators are implemented using microstrip technology and were designed at 2 GHz. These filters are specially built to be used in RF or any microwave applications systems.

The first topology made used of second coupled-line, coupled to the base cell was fabricated. The resonator was implemented using microstrip technology on FR4 substrate, with a chosen center frequency of 2 GHz. The characteristics of the substrate are given by: $\varepsilon_r = 5$, $h = 1.6$ mm and $tan\ \delta = 0.02$. The results of electromagnetic simulation and measurement are shown in Fig. 10. It can be seen that the measured resonant frequency in is slightly shifted from the simulated one, 2.14 GHz while two transmission zeros are found at 1.71 GHz and 2.57 GHz. The insertion loss is at 2 dB while the attenuation at $1.5f_o$ is 10dB. Fig. 11 illustrates the fabricated resonator for the first topology to prove the concept.
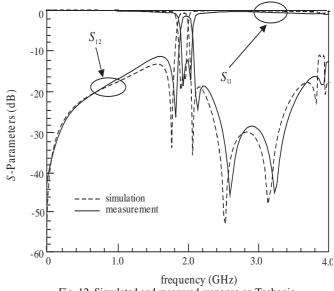
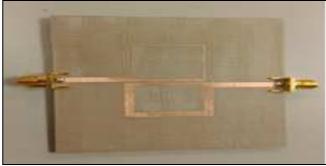

Fig. 12 Simulated and measured response on Tachonic

Fig. 13 Fabricated photo of the second topology: two closed-loops resonator

The second topology was implemented on Taconic substrate with a thickness of 1.64mm, relative dielectric constant (εr) of 4.5 and loss tangent of 0.0035 which is lower than FR-4 was used in implementing the second topology. The performance of the filter was measured and compared with simulated response, and the results are presented in Fig. 12. The measured results show that the two resonance frequencies are found at 1.945 GHz and 2.050 GHz while center frequency is positioned at 1.998 GHz giving a fractional bandwidth of 8.76 %.

Meanwhile, a transmission zeros was found at the lower stop-band occur at 1.840 GHz and two transmission zeros at the upper stopband occurred at 2.155 GHz and 2.610 GHz giving a passband bandwidth of 315 MHz. As such, the rejection level at the stopbands exceeded 24 dB while insertion loss and return loss are found at with 1.55 dB and 13.65 dB respectively. For proof of concept, the fabricated resonator is shown in Fig. 13.

The third topology was implemented on Taconic. The measured responses of the second and third resonators are compared as shown in Fig. 14. It was found that the fractional bandwidth of the third resonator had increased by 1.5% compared to the second resonator. The rejection level for both filters exceeding 30dB which is good performance.
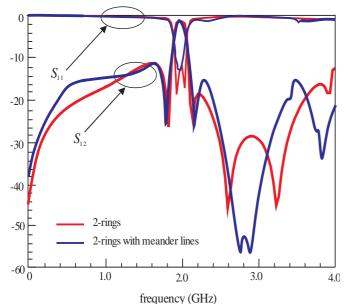
Fig. 14 Comparison of measured S-Parameters for 2nd order bandpass filters

Fig. 15 Fabricated photo of the third topology: Two closed-loops with meander lines resonators on Taconic microstrip substrate

The insertion loss of the third resonator has improved about 1.47% while the return loss exceeded 10dB compared to the second resonator. The fabricated filter size of the third topology was successfully reduced by 56.5% from the second topology. The fabricated photo of the third topology is shown in Fig. 15 as proof of concept. The size of the proposed filter is 5.3 cm x 3.25 cm. The length of the filter was successfully reduced more than half compared to the second topology.

Finally, all the responses for the three resonators are tabulated in Table 6. It can be seen that all the resonators had shown their own specific characteristics that are suitable for RF applications.

TABLE VI
COMPARISONS OF ALL THE RESONATORS' MEASURED RESPONSES

Topology	Topology 1 Closed-Loop with Second Coupled-Line	Topology 2 Closed-Loop with Coupled-Line	Topology 3 Closed-Loop Meander Lines
Microstrip substrate	FR-4 $\varepsilon_r = 4.1$ $h = 1.6$ mm $tan\delta$: 2×10^{-2}	Tachonic $\varepsilon_r = 4.5$ $h = 1.6$ mm $tan\delta$: 3.5×10^{-3}	
Insertion loss, dB	2.23	1.55	1.245
Fractional, BW (%)	18.93	8.76	10.23
Size	x = 79.51 y = 46.84	x = 71.66 y = 46.84	x = 52.84 y = 27.63

IV. CONCLUSION

In this paper, three pseudo-elliptic 2nd order bandpass resonator topologies were proposed based on the closed-loop resonator. All the topologies showed the advantages of high selectivity and prominent filter responses. The investigation of the resonators showed that the impedances of each resonator were optimized to obtain desired response by controlling the impedances of the closed-loops and the coupled-lines. Meanwhile, all the bandwidths of the resonators can be controlled by varying the gap in each resonator. Meander lines were introduced in the third topology to reduce the size and at the same time improved the response compared to the second topology. It has been proven in this work that meander structure [14], [15] enables the filter to be flexibly miniaturized, and this approach can be easily applied in various type coupled filters too. Finally, all the resonators were fabricated on microstrip substrates. The measured results had shown good agreement with the simulations while the filters demonstrated high selectivity, sharp rejection skirts and stopband attenuation levels above 24 dB.

In view of the experimental results, this arrangement scheme realized a filter not only with high selectivity and sharp skirt but also compact size, good performance and simple design at low cost. Therefore, these proposed topologies are suitable for advanced microwave communication applications that require spectral efficiency applications.

REFERENCES

[1] C. Z. Hua and W. Chao, "Design of stepped impedance resonator bandpass hairpin filter," in *Proc. ICEPT'16*, 2016, p. 1409.

[2] S. W. Ren, H. L. Peng, J. F. Mao, and A. M. Gao, "Compact quasi-elliptic wideband bandpass filter using cross-coupled multiple-mode resonator," *IEEE Microwave and Wireless Components Letters*, vol. 22, pp. 397-399, Aug. 2012.

[3] S. V. Kumar and A. R. Harish, "Dual mode bandpass filter using trefoil torus knot resonator," in *Proc. IEEE IMaRC'15*, 2015, p. 419.

[4] S. B. Cohn, "Parallel-couple transmission line resonator filter," *IRE Transactions on Microwave Theory and Techniques*, vol. 6, pp. 223-231, Apr. 1958.

[5] Z. Awang, *Microwave Systems Design*, Berlin, Germany: Springer, 2014.

[6] D. A. Letavin and V. A. Chechetkin," Miniature microwave bandpass filter with two circular spiral resonators," in *Proc. ICACCI'16*, 2016, p. 2315.

[7] R. Garg, I. Bahl, and M. Bozzi, *Microstrip Lines and Slotlines*, 3rd ed., London, UK: Artech House, 2013.

[8] A. Munir, "Development of dual-band microstrip bandpass filter based on split ring resonator," in *Proc. ICEAA'16*, 2016, p. 712.

[9] T. W. Kim, Y. J. Shin, and Y. S. Kim, "S-parameter characteristics of microstrip meander line," in *Proc. IEEK'08*, 2008, p. 1201.

[10] A. Khaleghi, "Dual band meander line antenna for wireless LAN communication," *IEEE Transactions on Antennas and Propagation*, vol. 55, pp. 1004-1009, Mar. 2007.

[11] T. Y. Xiang, T. Lei, and M. Peng, "Miniature dual mode bandpass filter based on meander loop resonator with source load coupling," in *Proc. APMC'15*, 2015, p. 1.

[12] K. G. Avanash and I. S. Rao," Design of compact meandered dual mode wideband microstrip bandpass filter using tuning stubs," in *Proc. ICMAP'15*, 2015, p. 1.

[13] N. A. Wahab, M. K. M. Salleh, Z. I. Khan, and E. A. Rashid, "Reconfigurable ring filter with controllable frequency response," *The Scientific World Journal*, vol. 2014, pp. 1-11, Jul. 2014.

[14] I. M. Yassin, A. Zabidi, M. S. A. M. Ali, N. M. Tahir, H. A. Hassan, H. Z. Abidin, and Z. I. Rizman, "Binary particle swarm optimization structure selection of nonlinear autoregressive moving average with exogenous inputs (NARMAX) model of a flexible robot arm," *International Journal on Advanced Science, Engineering and Information Technology*, vol. 6, pp. 630-637, Oct. 2016.

[15] M. N. M. Nor, R. Jailani, N. M. Tahir, I. M. Yassin, Z. I. Rizman, and R. Hidayat, "EMG signals analysis of BF and RF muscles in autism spectrum disorder (ASD) during walking," *International Journal on Advanced Science, Engineering and Information Technology*, vol. 6, pp. 793-798, Oct. 2016.